



# Thermal properties and crystal structures of cobalt(III)-cyclam complexes with the bis(trifluoromethanesulfonyl)amide anion (cyclam = 1,4,8,11-tetraazacyclotetradecane)

Oba, Yukiko

Mochida, Tomoyuki

---

(Citation)

Polyhedron, 99:275-279

(Issue Date)

2015-10-15

(Resource Type)

journal article

(Version)

Accepted Manuscript

(Rights)

© 2015 Elsevier.

This manuscript version is made available under the CC-BY-NC-ND 4.0 license  
<http://creativecommons.org/licenses/by-nc-nd/4.0/>

(URL)

<https://hdl.handle.net/20.500.14094/90002863>



# **Thermal properties and crystal structures of cobalt(III)–cyclam complexes with the bis(trifluoromethanesulfonyl)amide anion (cyclam = 1,4,8,11-tetraazacyclotetradecane)**

Yukiko Oba, Tomoyuki Mochida\*

*Department of Chemistry, Graduate School of Science, Kobe University, Rokkodai, Nada, Hyogo 657-8501, Japan*

## **ABSTRACT**

The bis(trifluoromethanesulfonyl)amide anion ( $[\text{Tf}_2\text{N}]^-$ ) has frequently been used as a component of ionic liquids. To investigate the effect of this anion and alkyl substituents on the thermal properties of macrocyclic metal complexes, cobalt(III) cyclam complexes  $[\text{Co}(\text{cyclam})\text{Cl}_2][\text{Tf}_2\text{N}]$  and its monoalkyl derivatives were prepared (cyclam = 1,4,8,11-tetraazacyclotetradecane). The corresponding hexafluorophosphate salts were also prepared and characterized. The salts with propyl and hexyl substituents melted at 171 °C and 153 °C, respectively, whereas other salts decomposed above 220 °C without melting. X-ray crystallography revealed the formation of intermolecular hydrogen bonds involving the NH hydrogens, which are responsible for the high melting points.

*Keywords:* Cyclam complex, Cobalt, Thermal analysis, Crystal structure, Hydrogen bond

---

\*Corresponding author Tel/fax: +81-78-803-5679,

*E-mail address:* tmochida@platinum.kobe-u.ac.jp (T. Mochida)

## 1. Introduction

Cyclam (1,4,8,11-tetraazacyclotetradecane) is a macrocyclic ligand with a rich coordination chemistry that has produced many versatile metal complexes [1–9]. Cyclam complexes have attracted interest in diverse areas related to medicine [3–5], catalysts [6–8], and ion sensors [9]. In this study, as part of our continuous study on the preparation of ionic liquids from metal complexes, we focused on the thermal properties of cyclam complexes. Ionic liquids are salts with melting points below 100 °C, and they have recently attracted much attention for both pure and applied science [10–16]. Several ionic liquids from metal-chelate complexes have been reported recently [17–21]. We prepared ionic liquids comprising cationic metal-chelate complexes and the bis(trifluoromethanesulfonyl)amide anion ( $[\text{Tf}_2\text{N}]^-$ ), which exhibit vapochromism, thermochromism, and the spin-crossover phenomenon [22, 23]. The melting points of these salts generally decrease upon using the  $[\text{Tf}_2\text{N}]^-$  anion and upon introducing alkyl substituents to the cation. Indeed, these modifications of Schiff base complexes [24] produced ionic liquids [22, 25]. There is also interest in the thermal properties of  $[\text{Tf}_2\text{N}]$  salts with chelate complexes [26]. In the present study, to investigate the effects of the anion and substituents on the thermal properties of cyclam complexes, we prepared the  $[\text{Tf}_2\text{N}]$  and hexafluorophosphate ( $[\text{PF}_6]^-$ ) salts of the cobalt cyclam complex and its *N*-monoalkyl derivatives  $[\text{Co}(\text{R-cyclam})\text{Cl}_2]\text{X}$  ( $\text{R} = \text{H}$  (**1**),  $\text{C}_3\text{H}_7$  (**2**),  $\text{C}_6\text{H}_{13}$  (**3**);  $\text{X} = [\text{Tf}_2\text{N}], [\text{PF}_6]$ ; Fig. 1). Examination of their thermal properties revealed that they exhibit very high melting points. However, the information obtained is useful for the molecular design of ionic liquids.

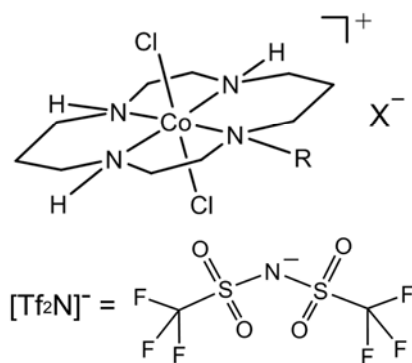


**Fig. 1.** Structural formula of  $[\mathbf{1}]\text{X}-[\mathbf{3}]\text{X}$  ( $\text{R} = \text{H}$  (**1**),  $\text{C}_3\text{H}_6$  (**2**),  $\text{C}_6\text{H}_{13}$  (**3**);  $\text{X} = [\text{Tf}_2\text{N}]$ ,  $[\text{PF}_6]$ ).

Structural formula of the  $[\text{Tf}_2\text{N}]^-$  anion is shown below.

## 2. Results and discussion

### 2.1. Preparation and thermal properties

$[\text{Co}(\text{R-cyclam})\text{Cl}_2]\text{Cl}$  was obtained by reacting cyclam derivatives and  $\text{CoCl}_2 \cdot 6\text{H}_2\text{O}$  under air. The hexafluorophosphate and  $[\text{Tf}_2\text{N}]$  salts were prepared by anion exchange from Cl salts using  $\text{NH}_4\text{PF}_6$  and  $\text{Li}[\text{Tf}_2\text{N}]$ , respectively. All the salts were obtained in the form of green solids.

The decomposition temperatures ( $T_{\text{dec}}$ ) determined by thermogravimetric (TG) analysis and melting points ( $T_{\text{m}}$ ) of the  $[\text{Tf}_2\text{N}]$  and hexafluorophosphate salts are summarized in Table 1. The TG traces are shown in Fig. S1 (supporting information).  $[\mathbf{2}][\text{Tf}_2\text{N}]$  and  $[\mathbf{3}][\text{Tf}_2\text{N}]$  melted at 171 °C and 153 °C, respectively, while  $[\mathbf{1}][\text{Tf}_2\text{N}]$  exhibited only decomposition without melting. Thus, elongation of the alkyl substituent decreased the melting points, but the melting points prove to be very high despite using the  $[\text{Tf}_2\text{N}]^-$  anion. The hexafluorophosphate salts decomposed above 220 °C without melting (Fig. S2). The decomposition temperatures of the  $[\text{Tf}_2\text{N}]$  and hexafluorophosphate salts were in the range 220–268 °C, and the thermal stability decreased in the order of  $[\mathbf{1}]\text{X} > [\mathbf{3}]\text{X} > [\mathbf{2}]\text{X}$  ( $\text{X} = [\text{Tf}_2\text{N}]$ ,  $[\text{PF}_6]$ ). The  $[\text{Tf}_2\text{N}]$  salts exhibited greater thermal stability than the hexafluorophosphate salts. All the salts exhibited continuous weight loss above the

decomposition temperatures.

**Table 1**

Decomposition temperatures ( $T_{\text{dec}}$ ), melting points ( $T_{\text{m}}$ ) and glass transition temperature ( $T_{\text{g}}$ ).

	$T_{\text{dec}}$ (°C) <sup>a</sup>	$T_{\text{m}}$ (°C) <sup>b</sup>	$T_{\text{g}}$ (°C) <sup>b</sup>
[1][Tf <sub>2</sub> N]	268	–	–
[2][Tf <sub>2</sub> N]	234	171	27
[3][Tf <sub>2</sub> N]	263	153	26
[1][PF <sub>6</sub> ]	259	–	–
[2][PF <sub>6</sub> ]	220	–	–
[3][PF <sub>6</sub> ]	228	–	–

<sup>a</sup> Determined by TG measurements (–3 wt%, 5 K min<sup>–1</sup>).

<sup>b</sup> Determined by DSC measurements (10 K min<sup>–1</sup>).

## 2.2. Differential scanning calorimetry

The thermal properties of [1][Tf<sub>2</sub>N]–[3][Tf<sub>2</sub>N] were investigated by differential scanning calorimetry (DSC). [1][Tf<sub>2</sub>N] exhibited no phase transitions between 123 K and 403 K. The DSC trace of [2][Tf<sub>2</sub>N] is shown in Fig. 2. This salt exhibited successive endothermic and exothermic peaks at around 80 °C only in the first heating cycle, independent of the scan rate (2–20 K min<sup>–1</sup>). They are probably transitions from an as-grown room-temperature phase (Phase I, Fig. 2) to a metastable phase, and then to a stable phase (Phase II). The stable phase exhibited no phase transition. Further heating led to melting at 171 °C ( $\Delta H = 38.6$  kJ mol<sup>–1</sup>,  $\Delta S = 87.0$  J K<sup>–1</sup> mol<sup>–1</sup>). After once melting, no crystallization occurred on cooling, and there was only a glass transition at 27 °C. The salt [3][Tf<sub>2</sub>N] melted at 153 °C during the heating process ( $\Delta H = 40.8$  kJ mol<sup>–1</sup>,  $\Delta S = 95.8$  J K<sup>–1</sup> mol<sup>–1</sup>). After melting and being allowed to cool, this liquid also exhibited only a glass transition at 26 °C. The DSC trace of this salt is shown in Fig. S3 (supporting information). The ratios of  $T_{\text{g}}/T_{\text{m}}$  for [2][Tf<sub>2</sub>N] and [3][Tf<sub>2</sub>N] are 0.68 and 0.70, respectively. They are in accordance with the empirical relationship  $T_{\text{g}}/T_{\text{m}} = 2/3$  [27], which generally holds for molecular liquids. The melting entropies of [2][Tf<sub>2</sub>N] and

[**3**][Tf<sub>2</sub>N] were comparable, although the conformational changes in the alkyl chains generally provide an entropy change of  $\sim 10.3 \text{ J K}^{-1} \text{ mol}^{-1}$  per methylene unit [28, 29].

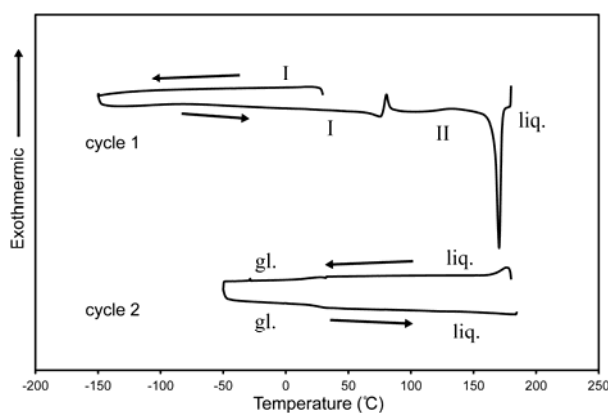


**Fig. 2.** DSC trace of [**2**][Tf<sub>2</sub>N] measured at  $10 \text{ K min}^{-1}$ .

### 2.3. Crystal structures

The crystal structures of [**1**][Tf<sub>2</sub>N], [**1**][PF<sub>6</sub>], and [**3**][Tf<sub>2</sub>N] were determined at room temperature. These salts crystallized in space groups  $P\bar{1}$ ,  $P2_12_12_1$ , and  $P2_1/c$ , respectively. All the NH hydrogens of the ligands form hydrogen bonds with neighboring anions or cations, forming network structures. The configurations of these complexes are regarded as *trans*-III according to the classification in the literature [30]. The anions in [**1**][Tf<sub>2</sub>N] and [**3**][Tf<sub>2</sub>N] exhibited the *cis*- and *trans*-conformation, respectively. In these salts, the nitrogen atoms in the anion exhibited two-fold disorder and the CF<sub>3</sub> moieties exhibited rotational disorder. This type of disorder has been often observed in salts with the [Tf<sub>2</sub>N]<sup>−</sup> anion. The hexafluorophosphate anion in [**1**][PF<sub>6</sub>] exhibited rotational disorder.

The packing diagrams and cation–cation arrangements of [**1**][Tf<sub>2</sub>N] and [**1**][PF<sub>6</sub>] are shown in Fig. 3a and 3b, respectively. They exhibit somewhat similar molecular arrangements, where two of the four NH hydrogens form hydrogen bonds with the chloride ligands of neighboring cations [N...Cl distances: 3.196(5) Å ([**1**][Tf<sub>2</sub>N]), 3.388(3) Å and 3.376(3) Å ([**1**][PF<sub>6</sub>)], and the other two with neighboring anions [N...O distances: 3.359(2) Å

(**1**)[Tf<sub>2</sub>N]); N...F distances: 3.074(8) Å and 3.112(9) Å (**1**)[PF<sub>6</sub>]]. The hydrogen bond distances between the cation and anion were shorter by 0.4 Å than the van der Waals contact distance, probably strengthened by electrostatic interactions. The cations form one-dimensional arrangements via double hydrogen bonds, which are further hydrogen-bonded with the anions to form network structures.

The packing diagrams and cation–cation arrangements of **3**[Tf<sub>2</sub>N] are shown in Fig. 3c. One of the three NH hydrogens in this salt forms a hydrogen bond with the chloride ligand of a neighboring cation (N...Cl distance: 3.339(2) Å), while the others form hydrogen bonds with the oxygen atoms of neighboring anions (N...O distance: 3.110(6) Å). The cation forms a dimer structure connected via the hydrogen bonds. The dimers form one-dimensional chains through the hydrogen bond with the anion.

The complexes prepared in the study exhibited very high melting points, despite the use of the [Tf<sub>2</sub>N]<sup>−</sup> anion and the introduction of alkyl substituents. This is probably owing to the hydrogen bond network. The melting points of **2**[Tf<sub>2</sub>N] and **3**[Tf<sub>2</sub>N] are due to the effect of the alkyl chain and a smaller number of hydrogen bonds, compared with **1**[Tf<sub>2</sub>N]. Therefore, it is expected that their melting points would decrease more by further alkylation of the NH hydrogens. In the cyclam complexes reported to date, the four NH hydrogens are also involved in hydrogen bonding. For example, [Cr(cyclam)Cl<sub>2</sub>]<sub>2</sub>Br has cation–cation and cation–anion hydrogen bonding similar to **1**[PF<sub>6</sub>] (N...Cl distance: 3.314 Å; N...Br distance: 3.475 Å) [31]. There are two salts of **1**, whose crystal structures have been reported: **1**Cl and **1**Cl·4H<sub>2</sub>O·0.47HCl, while their hydrogen bonding structures are different from those in the present salts. The chloride ion in the former salt, bridges four cations via hydrogen bond, having no hydrogen bond between the cations. The latter salt has cation–cation and cation–anion hydrogen bonds, and there are additional hydrogen bonds between the anion and the water molecule.

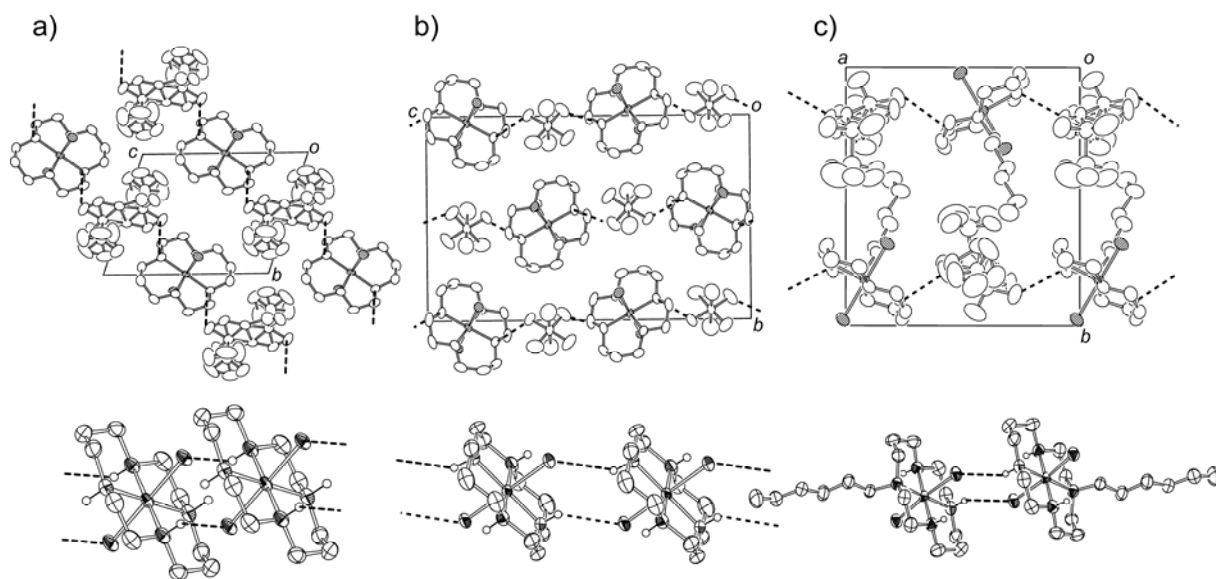


**Fig. 3.** The crystal structures of (a)  $[1][\text{Tf}_2\text{N}]$ , (b)  $[1][\text{PF}_6]$ , and (c)  $[3][\text{Tf}_2\text{N}]$ . The upper figures are packing diagrams and the lower figures cation–cation arrangements. Dotted lines indicate cation–anion and cation–cation hydrogen bonding. The metal center and chloride ligands are shaded in the packing diagrams.

### 3. Conclusions

Six new salts of cobalt(III) cyclam complexes with the  $[\text{Tf}_2\text{N}]^-$  and hexafluorophosphate anion were prepared. Most of the salts decomposed without melting, except for the  $[\text{Tf}_2\text{N}]$  salts of *N*-propyl and hexyl cyclam complexes. Although elongation of substituents decreased the melting points of the  $[\text{Tf}_2\text{N}]$  salts, the melting points of the cyclam complexes were proven to be intrinsically high. All the NH hydrogens in these salts form hydrogen bonds with neighboring cations and anions in the crystals; these bonds are probably responsible for the high melting points. This result suggests that further alkylation of NH hydrogens to inhibit hydrogen bonds may be effective for lowering the melting points of the designed ionic liquids. Considering the versatility of cyclam complexes, their liquefaction may lead to a variety of functional fluids. Investigation along this line is in progress in these laboratories.

## 4. Experimental

### 4.1. General

[Co(cyclam)Cl<sub>2</sub>]Cl was prepared according to a literature method [30]. Other reagents and solvents were commercially available. <sup>1</sup>H NMR spectra were recorded on a JEOL JNM-ECL-400 spectrometer. Infrared spectra were recorded on a Thermo Nicolet iS5 spectrometer equipped with a diamond ATR unit. DSC measurements were performed using a TA instruments Q100 differential scanning calorimeter at 10 K min<sup>-1</sup>, and at 2–20 K min<sup>-1</sup> when necessary. TG analysis was performed under nitrogen gas at a heating rate of 5 K min<sup>-1</sup> on a Rigaku TG8120.

### 4.2. Synthesis of ligands

#### 4.2.1. *N*-3-Propyl-1,4,8,11-tetraazacyclotetradecane (C<sub>3</sub>H<sub>7</sub>-cyclam)

The ligand was prepared based on the method used to prepare similar compounds [32]. Bromopropane (92 mg, 0.75 mmol) was added to a solution of cyclam (600 mg, 3 mmol) and trimethylamine (0.13 mL, 0.90 mmol) in chloroform (60 mL), and the solution was stirred at 45 °C under nitrogen gas for 3 d. The resulting mixture was washed ten times with 1 M sodium hydroxide aqueous solution and then washed three times with water, dried over MgSO<sub>4</sub>, and the solvent was evaporated at 50 °C to yield 150 mg of a yellow oil (80%, versus bromopropane). Unreacted cyclam could be recovered from the water layer [33]. <sup>1</sup>H NMR (400 MHz, CDCl<sub>3</sub>, TMS): δ = 0.87 (m, 3H), 1.47 (m, 2H), 1.71 (m, 3H), 2.36 (m, 3H), 2.49 (m, 4H), 2.60 (m, 4H), 2.67 (m, 3H), 2.73 (m, 7H).

#### 4.2.2 *N*-6-Hexyl-1,4,8,11-tetraazacyclotetradecane (C<sub>6</sub>H<sub>13</sub>-cyclam)

This ligand was prepared as described for C<sub>3</sub>H<sub>7</sub>-cyclam, using bromohexane (41 mg, 0.25 mmol) as a starting material, except that the reaction temperature was set at 55 °C. The

product obtained was yellow oil, and the yield was 58 mg (81%; versus bromohexane).  $^1\text{H}$  NMR (400 MHz,  $\text{CDCl}_3$ , TMS):  $\delta$  = 0.87 (m, 3H), 1.27 (m, 8H), 1.44 (s, 2H), 1.71 (m, 3H), 2.4 (m, 3H), 2.48 (m, 4H), 2.61(m, 4H), 2.68 (m, 3H), 2.73 (m, 7H).

### 4.3. Synthesis of cyclam complexes

#### 4.3.1 $[\text{Co}(\text{cyclam})\text{Cl}_2][\text{PF}_6]$ (**1**) $[\text{PF}_6]$ )

A saturated aqueous solution of  $\text{NH}_4\text{PF}_6$  (40 mg, 0.25 mmol) was added to a saturated aqueous solution of  $[\text{Co}(\text{cyclam})\text{Cl}_2]\text{Cl}$  (30 mg, 0.082 mmol), and stirred for 1 h. The resulting precipitate was collected by filtration and dried under vacuum. The product obtained was a light green powder, the yield was 37 mg (95%).  $^1\text{H}$  NMR (400 MHz,  $(\text{CD}_3)_2\text{SO}$ , TMS):  $\delta$  = 1.78 (q, 2H,  $J$  = 13.1 Hz), 1.99 (d, 2H,  $J$  = 14.8 Hz), 2.33–2.76 (m, 16H), 6.40 (br s, 4H). Anal. Calcd. for  $\text{C}_{10}\text{H}_{24}\text{Cl}_2\text{CoF}_6\text{N}_4\text{P}$ : C, 25.28; H, 5.09; N, 11.79. Found: C, 25.41; H, 5.25; N, 11.75. IR ( $\text{cm}^{-1}$ ) 555, 814, 834, 1028, 1061, 1102, 1135, 1295, 1320, 1430, 1465, 3210, 3250.

#### 4.3.2 $[\text{Co}(\text{cyclam})\text{Cl}_2][\text{Tf}_2\text{N}]$ (**1**) $[\text{Tf}_2\text{N}]$ )

A saturated aqueous solution of  $\text{Li}[\text{Tf}_2\text{N}]$  (70 mg, 0.25 mmol) was added to a saturated aqueous solution of  $[\text{Co}(\text{cyclam})\text{Cl}_2]\text{Cl}$  (30 mg, 0.082 mmol), and the solution was stirred for 1 h. The resulting precipitate was collected by filtration and dried under vacuum. The product obtained was a light green powder, and the yield was 48 mg (95%).  $^1\text{H}$  NMR (400 MHz,  $(\text{CD}_3)_2\text{SO}$ , TMS):  $\delta$  = 1.78 (q, 2H,  $J$  = 13.5 Hz), 1.99 (d, 2H,  $J$  = 15.8 Hz), 2.33–2.76 (m, 16H), 6.40 (br s, 4H). Anal. Calcd. for  $\text{C}_{12}\text{H}_{24}\text{O}_4\text{Cl}_2\text{CoF}_6\text{N}_5\text{S}_2$ : C, 23.62; H, 3.96; N, 11.48. Found: C, 23.85; H, 3.85; N, 11.47. IR (ATR Diamond,  $\text{cm}^{-1}$ ) 571, 614, 740, 764, 796, 890, 902, 1029, 1055, 1100, 1135, 1188, 1208, 1236, 1335, 1350, 1464, 3194, 3217, 3240.

#### 4.4. Synthesis of $C_3H_7$ -cyclam complexes

##### 4.4.1 $[Co(C_3H_7\text{-cyclam})Cl_2][PF_6]$ (**[2]** $[PF_6]$ )

$[Co(C_3H_7\text{-cyclam})Cl_2]Cl$  was prepared as described for  $[Co(cyclam)Cl_2]Cl$ , using  $C_3H_7$ -cyclam (55 mg, 0.22 mmol), except that a small amount of  $CHCl_3$  was added as the solvent to improve the solubility of the ligand. After adding water (1 mL) to the green powder of  $[Co(C_3H_7\text{-cyclam})Cl_2]Cl$ , MeOH was added to the suspension to dissolve the powder. A saturated aqueous solution of  $NH_4PF_6$  (113 mg, 0.69 mmol) was added to the solution and stirred for 1 h. The resulting solution was concentrated under reduced pressure to remove MeOH. The precipitate was collected by filtration, washed with water, and dried under vacuum. The product obtained was a green solid, and the yield was 53 mg (44%). The product was recrystallized by vapor diffusion of diethyl ether into an acetonitrile solution.  $^1H$  NMR (400 MHz,  $(CD_3)_2SO$ , TMS):  $\delta$  = 0.83 (t, 3H,  $J$  = 7.7 Hz), 1.51 (m, 1H), 1.65–1.82 (m, 3H), 1.98 (m, 3H), 2.25–3.01 (m, 19H), 3.12 (t, 1H,  $J$  = 12.6 Hz). Anal. Calcd. for  $C_{13}H_{30}Cl_2CoF_6N_4P$ : C, 30.19; H, 5.85; N, 10.83. Found: C, 30.36; H, 5.72; N, 11.04. IR ( $cm^{-1}$ ) 556, 590, 749, 829, 1035, 1066, 1089, 1103, 1293, 1385, 1428, 1460, 2978, 3210.

##### 4.4.2 $[Co(C_3H_7\text{-cyclam})Cl_2][Tf_2N]$ (**[2]** $[Tf_2N]$ )

A saturated solution of  $Li[Tf_2N]$  (81 mg, 0.28 mmol) in MeOH was added to a solution of **[2]** $[PF_6]$  (49.1 mg, 0.095 mmol) in MeOH–acetone and stirred for 1 h. The resulting solution was concentrated under reduced pressure, to which a small amount of  $CHCl_3$  was added, and the solution was washed three times with water. The organic layer was dried over anhydrous magnesium sulfate. After removing the solvent by evaporation, the residue was dissolved in  $CHCl_3$  and filtered. Addition of diethyl ether to the filtrate precipitated the product, which was dried under vacuum. The product obtained was a green solid, and the yield was 25 mg (40%).  $^1H$  NMR (400 MHz,  $(CD_3)_2SO$ , TMS):  $\delta$  = 0.83 (t, 3H,  $J$  = 7.7 Hz), 1.51 (m, 1H),

1.65–1.82 (m, 3H), 1.98 (m, 3H), 2.25–3.01 (m, 19H), 3.12 (t, 1H,  $J = 12.6$  Hz). Anal. Calcd. for  $C_{15}H_{30}O_4Cl_2CoF_6N_5S_2$ : C, 27.62; H, 4.63; N, 10.73. Found: C, 27.93; H, 4.90; N, 10.62. IR ( $cm^{-1}$ ) 569, 613, 652, 739, 761, 788, 825, 876, 898, 954, 972, 1022, 1035, 1048, 1100, 1135, 1177, 1354, 1349, 1428, 2360, 2941, 3224, 5892.

#### 4.5. Synthesis of $C_6H_{13}$ -cyclam complexes

##### 4.5.1 $[Co(C_6H_{13}\text{-cyclam})Cl_2][PF_6]$ (**[3]** $[PF_6]$ )

$[Co(C_6H_{13}\text{-cyclam})Cl_2]Cl$  was prepared as described for  $[Co(C_3H_7\text{-cyclam})Cl_2]Cl$ , using  $C_6H_{13}$ -cyclam (74 mg, 0.26 mmol). A saturated MeOH solution of  $Li[Tf_2N]$  (132 mg, 0.81 mmol) was added to a solution of  $[Co(C_6H_{13}\text{-cyclam})Cl_2]Cl$  in a mixture of water and MeOH, and the solution was stirred for 1 h. The resulting solution was evaporated under reduced pressure to remove the MeOH. The precipitate was collected by filtration, washed with water, and dried under vacuum. The product was recrystallized by vapor diffusion of diethyl ether into an acetonitrile solution. The product obtained was a green solid, and the yield was 77 mg (53%).  $^1H$  NMR (400 MHz,  $(CD_3)_2SO$ , TMS):  $\delta = 0.87$  (m, 3H), 1.29 (m, 8H), 1.44 (m, 1H), 1.56–1.84 (m, 2H), 1.88–2.07 (m, 2H), 2.2–2.80 (m, 17H), 2.89 (m, 2H), 3.11 (m, 1H). Anal. Calcd. for  $C_{16}H_{36}Cl_2CoF_6N_4P$ : C, 34.36; H, 6.49; N, 10.02. Found: C, 33.97; H, 6.77; N, 9.83. IR ( $cm^{-1}$ ) 556, 588, 828, 1039, 1052, 1066, 1101, 1422, 1461, 2926, 3243.

##### 4.5.2 $[Co(C_6H_{13}\text{-cyclam})Cl_2][Tf_2N]$ (**[3]** $[Tf_2N]$ )

The salt was prepared as described for **[2]** $[Tf_2N]$ , using **[3]** $[PF_6]$  (71 mg, 0.13 mmol). The green oil obtained was dissolved in ethanol, and vapor diffusion of hexane into this solution resulted in green crystals of the desired product. The yield was 33 mg (37%).  $^1H$  NMR (400 MHz,  $CDCl_3$ , TMS):  $\delta = 0.90$  (m, 3H), 1.30 (m, 8H), 1.93–2.21 (m, 6H), 2.43–2.56 (m, 2H), 2.64–3.19 (m, 17H). IR (ATR Diamond,  $cm^{-1}$ ) 570, 615, 652, 740, 762, 788, 892, 1031, 1050,

1100, 1135, 1181, 1351, 1458, 1463, 2360, 2934, 3240. Anal. Calcd. for  $C_{18}H_{36}O_4Cl_2CoF_6N_5S_2$ : C, 31.13; H, 5.22; N, 10.08, S, 9.23. Found: C, 31.18; H, 5.06; N, 10.24, S, 9.47.

#### 4.6. X-ray crystallography

X-ray diffraction data for **[1]**[Tf<sub>2</sub>N], **[1]**[PF<sub>6</sub>], and **[3]**[Tf<sub>2</sub>N] were collected on a Bruker APEX II Ultra CCD diffractometer using MoK $\alpha$  radiation ( $\lambda = 0.71073$  Å) at room temperature. Single crystals of **[1]**[Tf<sub>2</sub>N] and **[1]**[PF<sub>6</sub>] were obtained by vapor diffusion of diethyl ether into acetonitrile solutions, while those of **[3]**[Tf<sub>2</sub>N] were obtained by vapor diffusion of hexane into an ethanol solution. The crystallographic parameters are listed in Table 2. The structures were determined by direct methods using SHELX-97 [34], and ORTEP-3 [35] was used to generate the molecular graphics.

#### Appendix A. Supplementary data

Supplementary material associated with this article can be found at doi: 10.1016/j.poly.XXXXXX. CCDC 1061375 (**[1]**[Tf<sub>2</sub>N]), 1061376 (**[1]**[PF<sub>6</sub>]), and 1061374 (**[3]**[Tf<sub>2</sub>N]) contains the supplementary crystallographic data for this paper. These data can be obtained free of charge via <http://www.ccdc.cam.ac.uk/conts/retrieving.html>, or from the Cambridge Crystallographic Data Centre, 12 Union Road, Cambridge CB2 1EZ, UK; fax: (+44) 1223-336-033; or e-mail: [deposit@ccdc.cam.ac.uk](mailto:deposit@ccdc.cam.ac.uk).

#### Acknowledgments

We thank H. Hosokawa for discussion and for his help with structural determination by X-ray. This work was supported by KAKENHI (No. 24350073) from the Japan Society for the Promotion of Science.

**Table 2**Crystallographic parameters for [1][Tf<sub>2</sub>N], [1][PF<sub>6</sub>], and [3][Tf<sub>2</sub>N]

	[1][Tf <sub>2</sub> N]	[1][PF <sub>6</sub> ]	[3][Tf <sub>2</sub> N]
Empirical formula	C <sub>12</sub> H <sub>24</sub> Cl <sub>2</sub> CoF <sub>6</sub> N <sub>5</sub> O <sub>4</sub> S <sub>2</sub>	C <sub>10</sub> H <sub>24</sub> Cl <sub>2</sub> CoF <sub>6</sub> N <sub>4</sub> P	C <sub>18</sub> H <sub>36</sub> Cl <sub>2</sub> CoF <sub>6</sub> N <sub>5</sub> O <sub>4</sub> S <sub>2</sub>
Formula weight	610.31	475.13	694.47
Crystal system	Triclinic	Orthorhombic	Monoclinic
Space group	<i>P</i> -1	<i>P</i> 2 <sub>1</sub> 2 <sub>1</sub> 2 <sub>1</sub>	<i>P</i> 2 <sub>1</sub> /c
<i>a</i> (Å)	6.388(2)	6.4084(7)	13.4725(15)
<i>b</i> (Å)	9.115(3)	13.2962(15)	11.9853(13)
<i>c</i> (Å)	11.206(4)	21.037(2)	18.375(2)
$\alpha$ (°)	104.395(4)	90	90
$\beta$ (°)	98.367(4)	90	100.8690(10)
$\gamma$ (°)	110.387(4)	90	90
Volume (Å <sup>3</sup> )	572.8(4)	1792.5(3)	2913.9(6)
<i>Z</i>	1	4	4
<i>d</i> <sub>calcd.</sub> (g cm <sup>-3</sup> )	1.769	1.761	1.583
$\lambda$ (Å)	0.71073	0.71073	0.71073
$\mu$ (mm <sup>-1</sup> )	1.243	1.404	0.988
<i>T</i> (K)	296	292	296(2)
<i>F</i> (000)	310	968	1432
Reflections collected	2881	10294	15634
Independent reflections	2173 ( <i>R</i> <sub>int</sub> = 1.69%)	4080 ( <i>R</i> <sub>int</sub> = 4.83%)	6159 ( <i>R</i> <sub>int</sub> = 2.24%)
Completeness to $\theta$ (%)	96.7	99.9	99.6
Parameters	197	270	438
Goodness-of-fit on <i>F</i> <sup>2</sup>	1.027	0.805	1.023
<i>R</i> <sub>1</sub> <sup>a</sup> , <i>wR</i> <sub>2</sub> <sup>b</sup> ( <i>I</i> > 2 $\sigma$ ( <i>I</i> ))	0.0294, 0.0786	0.0366, 0.1028	0.0333, 0.0931
<i>R</i> <sub>1</sub> <sup>a</sup> , <i>wR</i> <sub>2</sub> <sup>b</sup> (all data)	0.0315, 0.0812	0.0384, 0.1051	0.0397, 0.0981
Largest diff. peak and hole (e Å <sup>-3</sup> )	0.458 and -0.439	0.484 and -0.799	0.557 and -0.475

<sup>a</sup>  $R_1 = \sum ||F_o| - |F_c|| / \sum |F_o|$ , <sup>b</sup>  $wR_2 = [\sum w (F_o^2 - F_c^2)^2 / \sum w (F_o^2)^2]^{1/2}$

## References

- [1] E. H. S. Sousa, C. P. Oliveira, L. C. G. Vasconcellos, L. G. F. Lopes, I. C. N. Diogenes, I. M. M. Carvalho, J. C. V. Miranda, F. A. Dias, I. S. Moreira, *Thermochim. Acta*, **376**, 141–145 (2001).
- [2] F. Létumier, G. Broeker, J. Barbe, R. Guillard, D. Lucas, V. Dahaoui-Gindrey, C. Lecomte, L. Thouin, C. Amatore, *J. Chem. Soc., Dalton Trans.*, 2233–2239 (1998).
- [3] A. D. Ostrowski, R. O. Absalonson, M. A. De Leo, G. Wu, J. G. Pavlovich, J. Adamson, B. Azhar, A. V. Iretskii, I. L. Megson, P. C. Ford, *Inorg. Chem.*, **50**, 4453–4462 (2011).
- [4] X. Liang, P. J. Sadler, *Chem. Soc. Rev.*, **33**, 246–266 (2004).
- [5] A. J. Gomes, E. M. Espreafico, E. Tfouni, *Mol. Pharmaceutics*, **10**, 3544–3554 (2013).
- [6] S. Matsuoka, K. Yamamoto, T. Ogata, M. Kusaba, N. Nakashima, E. Fujita, S. Yanagida, *J. Am. Chem. Soc.*, **115**, 601–609 (1993).
- [7] S. Olivero, J.-P. Rolland, E. Duñach, *Organometallics*, **17**, 3747–3753 (1998).
- [8] J. Cho, S. Jeon, S. A. Wilson, L. V. Liu, E. A. Kang, J. J. Braymer, M. H. Lim, B. Hedman, K. O. Hodgson, J. S. Valentine, E. I. Solomon, W. Nam, *Nature*, **478**, 502–505 (2011).
- [9] E. Tamanini, K. Flavin, M. Motevalli, S. Piperno, L. A. Gheber, M. H. Todd, M. Watkinson, *Inorg. Chem.*, **49**, 3789–3800 (2010).
- [10] R. D. Rogers, K. R. Seddon (Eds.). *Ionic Liquid: Industrial Applications to Green Chemistry*, Vol. 818, American Chemical Society, ACS Symposium Series, Washington, D. C. (2002).
- [11] A. Stark, K.R. Seddon. In *Kirk-Othmer Encyclopedia of Chemical Technology*, K. Othmer (Ed.), Vol. 26, 5<sup>th</sup> Edn, pp. 836–919, Wiley-Interscience, New York (2007).
- [12] I. J. B. Lin, C.S. Vasam. *J. Organomet. Chem.*, **690**, 3498–3512 (2005).
- [13] S.-G. Lee. *Chem. Commun.*, **42**, 1049–1063 (2006).

- [14] M. Armand, F. Endres, D.R. MacFarlane, H. Ohno, B. Scrosati. *Nat. Mater.*, **8**, 621–629 (2009).
- [15] M. Pucheault, M. Vaultier. *Top. Curr. Chem.*, **290**, 83–126 (2009).
- [16] T. Torimoto, T. Tsuda, K. Okazaki, S. Kuwabata. *Adv. Mater.*, **22**, 1196–1221 (2010).
- [17] M. Iida, S. Kawakami, E. Syouno, H. Er, E. Taguchi, *J. Colloid Interface Sci.*, **356**, 630–638 (2011).
- [18] Y. Song, H. Jing, B. Li, D. Bai, *Chem. Eur. J.*, **17**, 8731–8738 (2011).
- [19] C. Li, W. -T. Wong, *Tetrahedron Lett.*, **43**, 3217–3220 (2002).
- [20] T. Tamura, K. Yoshida, T. Hachida, M. Tsuchiya, M. Nakamura, Y. Kazue, N. Tachikawa, K. Dokko, M. Watanabe, *Chem. Lett.*, **39**, 753–755 (2010).
- [21] A. Branco, L. C. Branco, F. Pina, *Chem. Commun.*, **47**, 2300–2302 (2011).
- [22] M. Okuhata, Y. Funasako, K. Takahashi, Y. Mochida. *Chem. Commun.*, **49**, 7662–7664 (2013).
- [23] Y. Funasako, T. Mochida, K. Takahashi, T. Sakurai, H. Ohta, *Chem. -Eur. J.*, **18**, 11929–11936 (2012).
- [24] M. Okuhata, T. Mochida, *Polyhedron*, **43**, 153–158 (2012).
- [25] M. Okuhata, T. Mochida, *J. Coord. Chem.*, **67**, 1361–1366 (2014).
- [26] T. Huxel, M. Skaissgirski, J. Klingele, *Polyhedron*, **93**, 28–36 (2015).
- [27] O. Yamamuro, Y. Minamimoto, Y. Inamura, S. Hayashi, H. Hamaguchi, *Chem. Phys. Lett.*, **423**, 371–375 (2006).
- [28] R. L. Gardas, M. G. Freire, P. J. Carvalho, I. M. Marrucho, I. M. A. Fonseca, A. G. M. Ferreira, A. G. M. Ferreira, J. A. P. Coutinho, *J. Chem. Eng. Data*, **52**, 80–88 (2007).
- [29] Y. Shimizu, Y. Ohte, Y. Yamamura, K. Saito, *Chem. Phys. Lett.*, **470**, 295–299 (2009).
- [30] B. Bosnich, C. K. Poon, M. L. Tobe, *Inorg. Chem.*, **4**, 1102–1108 (1965).
- [31] C. G. Dealwis, R. W. Janes, R. A. Palmer, J. N. Lisgarten, D. Maes, C. D. Flint, D. M.

Gazi, *Acta Cryst.*, **C48**, 1754–1756 (1992).

[32] C. Li, W. -T. Wong, *Tetrahedron Lett.*, **43**, 3217–3220 (2002).

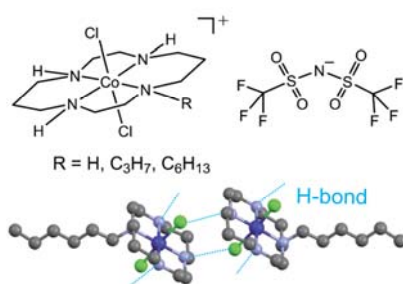
[33] J. Massue, S. E. Plush, C. S. Bonnet, D. A. Moore, T. Gunnlaugsson, *Tetrahedron. Lett.*, **48**, 8052–8055 (2007).

[34] G. M. Sheldrick, *Acta Cryst.*, **D64**, 112–122 (2008).

[35] L. J. Farrugia, *J. Appl. Cryst.*, **32**, 837–838 (1999).

## Synopsis

Salts comprising cationic cobalt(III)-cyclam complexes and the bis(trifluoromethanesulfonyl)amide anion ( $[\text{Tf}_2\text{N}]^-$ ) were prepared, and their thermal properties and crystal structures investigated. They exhibited very high melting points despite the introduction of alkyl substituents, which was ascribed to the presence of intermolecular hydrogen bonds in the crystals.



## Electronic supporting information

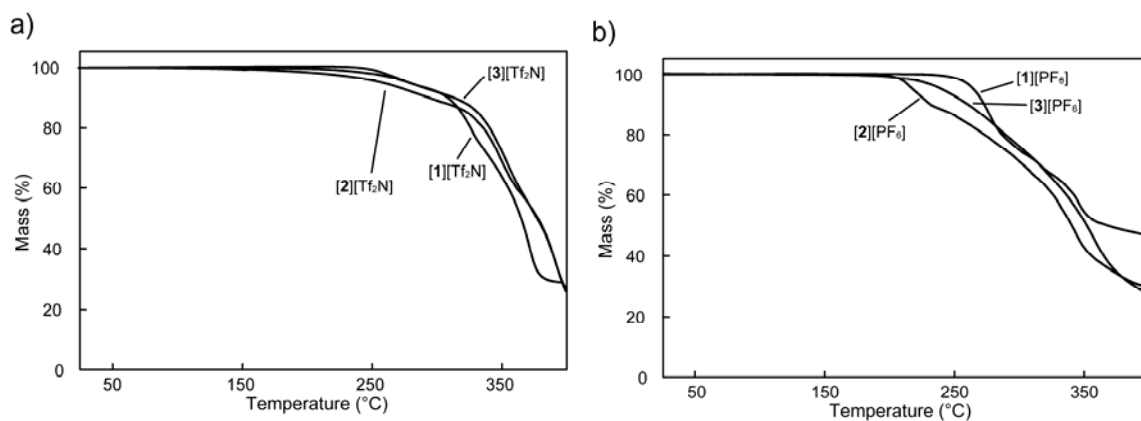


**Fig. S1.** Thermogravimetric traces of (a)  $[\text{Tf}_2\text{N}]$  salts and (b)  $[\text{PF}_6]$  salts.

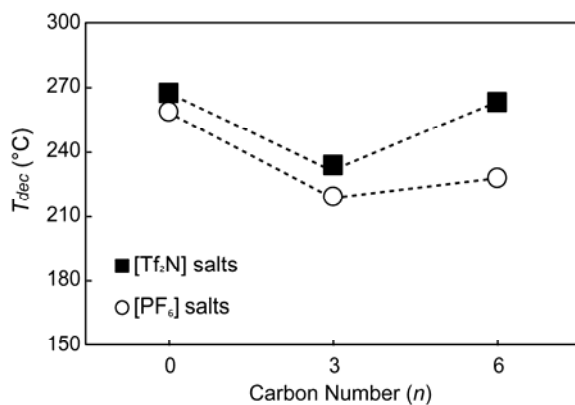


**Fig. S2.** Decomposition temperatures of the  $[\text{PF}_6]$  ( $\circ$ ) and  $[\text{Tf}_2\text{N}]$  ( $\blacksquare$ ) salts plotted vs. carbon number in the substituent.

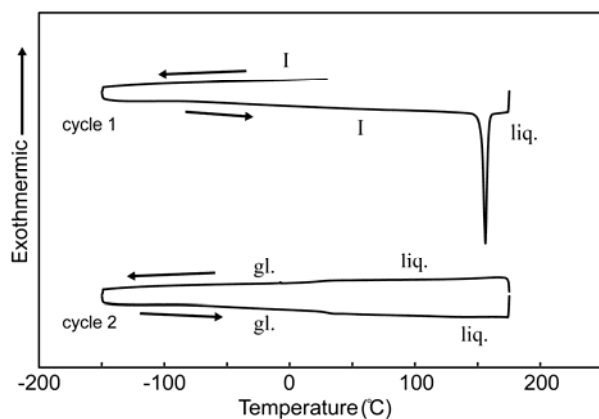


**Fig. S3.** DSC trace of  $[\mathbf{3}][\text{Tf}_2\text{N}]$  measured at  $10 \text{ K min}^{-1}$ .